"The final publication is available at link.springer.com"
DOI: 10.1007/s00216-015-8506-8
ANALYTICAL AND BIOANALYTICAL CHEMISTRY 407(10): 2887-2898

Quantitative Determination of Coenzyme Q_{10} from Dietary Supplements by FT-NIR Spectroscopy and Statistical Analysis

Anita Rácz[1,2], Andrea Vass[2], Károly Héberger[1,*], Marietta Fodor[2]

[1] Research Centre for Natural Sciences, Hungarian Academy of Sciences, Institute of Materials and Environmental Chemistry, Department of Plasma Chemistry

H-1117 Budapest XI., Magyar Tudósok krt. 2.

[2] Corvinus University of Budapest, Faculty of Food Science, Department of Applied Chemistry,

H-1118 Budapest XI., Villányi út 29-43.

* To whom correspondence should be sent:

E-mail address: heberger.karoly@ttk.mta.hu (Károly Héberger)

Phone: +36 1 382 6509

Abstract

A novel, time- and money-sparing method has been developed and validated for the quantitative determination of coenzyme Q10 (CoQ10) from several dietary supplements. FT-NIR spectroscopy was applied for the examination, and a calibration model was built by partial least-square regression (PLS-R) using fifty dietary supplements. The combination of FT-NIRS and multivariate calibration methods is a very fast and simple way to replace the commonly used HPLC-UV method; because in contrast with the traditional techniques sample pretreatment and reagents are not required and no wastes are produced.

The calibration models could be improved by different variable selection techniques (for instance interval PLS, interval selectivity ratio, genetic algorithm), which are very fast and user-friendly. The R^2 (goodness of calibration) and Q^2 (goodness of validation) of the variable selected models are highly increased, the R^2 values being over 0.90 and the Q^2 values being over 0.86 in every case. Five-fold cross-validation and external validation were applied. The developed method(s) could be used by quality assurance laboratories for routine measurement of coenzyme Q10 products.

Keywords: coenzyme Q10, dietary supplement, FT-NIRS, multivariate calibration, PLS, variable selection

Introduction

Coenzyme Q10 (CoQ10) or ubiquinone is a lipid-soluble benzoquinone where Q refers to the quinone chemical group, and 10 refers to the number of isoprenyl units in the side chain. CoQ10 is the component of mitochondrial respiratory chain and plays an important role in the electron transport. Ubiquinone is not just a coenzyme but also an antioxidant in its reduced form (ubiquinol) [1]. CoQ10 in reduced and oxidized form occurs in cellular membranes, for example blood serum or serum lipoproteins, but its quantity decreases with aging. This is one the most common nutrients nowadays, which is the active substance of several dietary supplements.

The reason of the wide popularity of CoQ10 is that it could help in prevention and treatment of many diseases, such as mitochondrial disease [2] and breast cancer [3] and it can decrease oxidative stress and increase antioxidant enzyme activity in patients with coronary artery disease [4]. Other studies suggest that CoQ10 may improve the ejection fraction in patients with congestive heart failure [5]. The oral CoQ10 may also improve functional capacity, and endothelial function in chronic heart failure [6] without any side effects. G. López-Llunch *et. al*. published that coenzyme Q is a key factor in the aging process and the maintenance of this nutrient is a good strategy to preserve health during aging [7]. CoQ10 is obtained from meat, poultry, fish and rapeseed oil, but if one needs a larger amount, many dietary supplements are commercially available for costumers [8].

In the last few years the number of CoQ10 dietary supplements has increased rapidly, thus the quality assurance of these products is very important. The commonly used techniques for the measurement of CoQ10 in different matrices are summarized in **Table 1** [9–16].

Table 1

The most common techniques were the different HPLC methods, but these are expensive, time-consuming and sample pretreatment is needed. Therefore, the aim of our work was to develop an FT-NIRS method for the determination of CoQ10 concentration. The FT-NIRS technique has a long tradition in food, agricultural and pharmaceutical chemistry, because it is a cheap, rapid and

non-destructive analytical method to quantify different materials. There are numerous publications, which use near-infrared technique or the combination of NIRS with multivariate calibration methods (most often multiple linear regression (MLR), principal component regression (PCR) and partial least-square regression (PLS-R) for quality assurance [17–20]. H. Huang *et. al*. summarized the examinations and possibilities of NIRS for on/in/at-line monitoring of quality in food and beverages [21]. M. Cocchi *et. al.* gave a good example for the application of NIRS with calibration methods to adulteration problems [22].

Material and methods

Samples

Fifty-two commercially available CoQ10 dietary supplements (between 8-120 mg/g CoQ10 content) were obtained from BioCo Magyarország company and analyzed in the form of tablets and hard capsules. The reference measurement was HPLC-UV method for the samples' FT-NIRS analysis.

HPLC reference measurements – reagents and apparatus

Acetonitrile (ACN; HPLC grade) was purchased from Scharlau (Barcelona, Spain). Tetrahydrofuran (THF; isocratic HPLC grade), 0.45 μm Polytetrafluoroethylene PTFE syringe filters were ordered from VWR (Radnor, PA, USA). The standard coenzyme Q10 (≥98%) was obtained from the Sigma–Aldrich group (Schnelldorf, Germany). $FeCl_3$ (≥99%) were ordered from Reanal (Budapest, Hungary). Ultra-pure water (18.2 MΩcm) was obtained from a Milli-Q system from Merck-Millipore (Milford, MA, USA).

For the determination of total Q10 content an Agilent 1200 HPLC (Agilent Technologies) system was used and the chromatography was executed in isocratic mode on an Agilent Zorbax XDB C_{18} HPLC column (2.1 mm × 50 mm × 3.5 μm) followed by UV detection at 275 nm. The column

temperature was set to 30 °C. The eluent consisted of the mixture of ACN: THF:water in 65:30:5 % v/v rate and the flow rate was 0.35 ml min^{-1}. The injection volume was 10 µl. The sample preparation was assisted with an ultrasonic bath (type T2MODX; VWR), and with a horizontal shaking table (T2125; MTA Kutesz, Budapest, Hungary) operated at 400 RPM. The limit of quantitation (LOQ) for HPLC-UV method was 0.05 mg Q10/g.

Sample preparation

The only sample pretreatment for FT-NIRS analysis was the careful homogenization of tablets and the content of encapsulated products in a mortar.

For HPLC-UV analysis the capsules of all encapsulated products were removed right before the sample preparation process; the contents of 10 capsules pooled and homogenized. Tablets were ground in a mortar to provide adequate homogeneity. The procedure was based on the AOAC Official Method 2008.07 [13] and later optimized [23]. The exact method is as follows: 200 mg of the homogenized samples were extracted in dark 25 ml volume flash with 20.0 ml extraction mixture containing ACN:THF:water in 40:55:5 % v/v rate in two steps, first shaking for 30 minutes on a shaking table, then using sonication in an ultrasonic bath for an additional 30 minutes. The solutions were made up with the extraction mixture to 25.0 ml. 1 ml $FeCl_3$ (1.0 mg ml^{-1} diluted in ethanol) was added to 1.0 ml aliquot from each extract using in 10 ml dark volume flasks. The mixtures were vortex mixed, left incubating for 30 min at room temperature. Finally, the solutions were made up to 10.0 ml with HPLC-UV eluent (ACN:THF:water in 60:35:5 % v/v rate). The solutions were then filtered through 0.45 µm PTFE syringe filters and injected to the HPLC-UV instrument. The total CoQ10 concentration was quantified by external calibration with peak area integration. Calibrations points were set to 25.0, 50.0, 75.0, 100.0 and 125.0 µg CoQ10 ml^{-1}, respectively.

FT-NIRS measurements

Bruker MPA^{TM} Multipurpose FT-NIR analyzer (Bruker Optik GmbH, Ettlingen, Germany) was used for FT-NIRS measurements. The device is equipped with a quartz beam splitter; an integrated Rocksolid^{TM} interferometer; a rotatable sample wheel; a PbS detector working in the 800–2700 nm wavelength range (12800-3600 cm^{-1} wavenumber). OPUS 6.5 (Bruker Optik GmbH, Ettlingen, Germany) software was integrated as a device manager. Diffuse reflectance mode was used for the collection of absorption spectra. The spectral resolution was 8 cm^{-1}, the scanner speed was 10 kHz and each spectrum was the average spectrum of 32 subsequent scans. The integrated gold coated surface of the integrating sphere was used for measuring internal background. Every sample had two duplicates and each duplicate was measured twice. The average of the duplicates' spectra was used for the multivariate calibration.

Statistical analysis – Partial least-squares regression (PLS-R)

The PLS-R is one of the most common multivariate statistical methods, which is very close to linear regression, principal component analysis and principal component regression. The method develops a mathematical connection between the measured independent (**X**) variables (for example wavelengths) and dependent (**Y**) variable(s) (reference values). The basic idea of PLS regression is a matrix transformation, which divides the original **X** and **Y** data matrices to the multiplication of score and loading matrices:

$$\mathbf{X} = \mathbf{TP'} + \mathbf{E} \quad (1)$$

$$\mathbf{Y} = \mathbf{UQ'} + \mathbf{F^*} \quad (2)$$

where **E**, **F*** are the error matrices and if all components are utilized, **E**=**F*=0**.

There is a linear relation between **X** and **Y** matrices: **Y**=**X***b*, where *b* is the regression coefficient which comes from the so called inner relationship of **T** and **U** matrices [24].

PLS components (latent variables) are defined by the regression model. The number of used PLS components is very important, because the measured data always contains noise and the

components which have less importance often suppress the systematic information. It could also be a problem when the number of PLS components is too high or too low. In the first case, the model will be overfitted, whereas in the latter case the model will be underfitted. In this study the number of PLS components was chosen by the built-in algorithm of Unscrambler software (global minimum of the root mean squared error).

Statistical analysis – variable selection

1. Interval PLS method (iPLS)

The iPLS method is a very common choice for variable selection especially in the case of near-infrared spectra and NMR spectra because spectral data are highly correlated and the usage of variable windows is a better option than examination of each variable individually [25–28]. This technique is very similar to the original PLS method, but here the spectra are divided into a number of intervals (equal length or manually made intervals). The number of intervals is usually 10, 20 or 40, but it is optional for every case. PLS models are made for each interval and the aim of the method is to choose those one or few intervals, which have the smallest root mean squared error of cross-validation (RMSECV), root mean squared error of calibration RMSEC or the highest R^2 (goodness of calibration), Q^2 (goodness of validation) values. The use of these intervals gives better prediction instead of using the whole spectra.

2. Interval Selectivity Ratio (iSR)

The basic idea of this method is developed by T. Rajalahti *et al.* [29]. The selectivity ratio can be calculated for each spectral variable with the following equation:

$$SR_i = v_{exp,i} / v_{res,i} \text{ , where } i = 1, 2, 3 \ldots m \quad (3)$$

Where v_{exp} (R^2) is the explained variance and v_{res} (SEC) is the residual variance. The original equation of selectivity ratio was slightly modified, introducing a square root in the denominator. A

simple algebraic transformation (square root or division by the same number – the degree of freedom) does not change the tendencies observed. We modified the equation for spectral intervals:

$$SR_i = R_i^2/RMSEC_i$$, where i = 1, 2, 3 … m (m is the number of intervals) (4)

In this study interval SR was used for the same reasons as iPLS method. In the latter equation degree of freedom is not used for R^2, but this equally influences all intervals. The higher the selectivity ratio is, the higher the importance of the interval.

3. Genetic Algorithm (GA)

This method is searching for the global minimum, but it is just approaching the global one. The initial step is the random choice of the amount of variables. In such a way the size of the population is defined. It is usually between 20 and 500 [25, 30]. The following steps are the reproduction, cross-over and mutation. The whole process is repeated until the stop criterion is reached. Stop criterion can be reached when the minimum criterion is satisfied, but there can be other stop criteria, for example the predefined number of generations or predefined time of elaboration. GA also has the opportunity to use variable windows. In PLS toolbox application the maximum number of variable in one window is 50. In this study variable windows are used for the genetic algorithm. It is also necessary here, because there are too many variables and they are correlated.

Statistical analysis – Sum of ranking differences (SRD) method for comparison of models

The sum of ranking differences is a novel method [31–33] to compare models and it is entirely general. In the input matrix the samples are arranged in the rows and the models (variables) are arranged in the columns. In the first step the samples in every column are ranked by increasing magnitude. Then, the difference between the rank of the method and the rank of the known reference (benchmark) is computed. If the benchmark is not known, the average, minimum or

maximum can be used instead. In the last step, the absolute values of the differences are summed together for all methods to be compared. The closer the SRD value is to zero, the better the method. SRD is validated by a randomization test and a bootstrap like cross-validation.

Results and discussion

Initially fifty-two dietary supplements were measured by FT-NIR spectroscopy in the range of 12800-3600 cm^{-1} (800-2700 nm). The average of each samples' spectra was used for the further statistical analysis. The part of the spectra between 12800 cm^{-1} and 9000 cm^{-1} (800-1111 nm) was cut, because it didn't carry any systematic information. The first step before the building of the calibration model is the outlier detection. There were two spectral outliers, which were clearly differing from the average one (**Figure 1**). Principal component analysis (STATISTICA 12® Statsoft, Tulsa, Oklahoma, USA) was used as a verification method in spectral outlier detection. The PCA result (**Figure 2**) confirms us that the samples - namely Av5 and 9539 - are separable from the other samples (out of the 99 % confidence interval).

Figure 1

Figure 2

Tracking out the reasons for outlying observations we established that these two samples were mixed with other vitamins in high concentration, which could interfere with their spectra.

The calibration models were created in Unscrambler version 9.7 (CAMO Software, Oslo, Norway). The first model was made for the original dataset, which contains fifty samples and the whole spectrum range (between 9000-3600 cm^{-1}). Data pretreatment had not been applied at first because we wanted to study the effect of the various scaling methods as well. As we will see later none of the data scaling methods gave much better results. These models are summarized in **Table 2** in the discussion. HPLC concentrations were used as reference (measured **Y** values). Seven PLS components were used for the calibration model. **Figure 3** shows the predicted **Y** values against the measured **Y** values. The R^2 value was 0.85 for the calibration (marked blue) and the Q^2 value was

0.71 for the validated model (marked red). The root mean squared error for the calibration (RMSEC) was 11.26 (mg/g) and 15.74 (mg/g) for the cross-validation (RMSECV). Five-fold cross-validation with randomized sample selection (randomly selected five equal groups) was used as the validation method here and also in the following cases.

Figure 3

In the next few cases calibration models were created with data pretreatment and different variable selection methods.

The result of iPLS

Because the calibration model cannot be considered as perfect, we wanted to improve it with fewer variables. The iPLS method helps us to choose which variable has a bigger importance in the creation of the calibration model. The first time the dataset was divided into ten parts, but it was not sufficient; the variables formed too large groups. In the second case the dataset was divided into 20 parts and it was appropriate for further analysis. iPLS was used for the dataset without any scaling method and it was separated into 20 parts. A PLS regression model was built for each part separately. RMSEC and RMSECV values were calculated for the regression models. Finally, RMSECV values were plotted against the intervals, which could help us to choose those few parts of the variables which are the most important (have the lowest RMSECV values) for the calibration model. **Figure 4** plots RMSECV values against the wavelength-intervals; the RMSECV values for the whole spectra and the average spectra are also plotted on the graph.

Figure 4

Five nearby intervals (350 variables) were chosen (6303 – 4953 cm^{-1} = 1587 – 2019 nm) for the calibration model. The inclusion of the last interval -which has somewhat larger RMSECV value - is justified by the higher R^2 value and the shape of the important band of the spectra. Before the creation of the calibration model, first derivatives as scaling for data pretreatment were applied. Seven PLS components were selected. On **Figure 5** the R^2 value was 0.92 for the calibration

(marked blue) and the Q^2 value was 0.87 for the validated model (marked red). The RMSEC value for the calibration was 8.16 and the RMSECV value for the validation was 10.58 (mg/g). This model is much better than the original one. Especially in the case of the validated model, the Q^2 value was increased from 0.71 to 0.87. The selected spectra areas can be assigned to functional groupings and bonds (methyl antisymmetric and symmetric C-H stretching vibrations, methylene antisymmetric and symmetric C-H stretching vibrations, trisubstituted alkene C-H stretching vibrations, 1,4-Quinones group) [34, 35].

Figure 5

The result of iSR

Interval selectivity ratio is also used as variable selection method. The same 20 intervals were applied here as in the case of iPLS. The RMSECV and R^2 values are used for the calculation of the selectivity ratio of each interval (Eq. (4)). Each selectivity ratio value was plotted against the intervals of the variables and the wavenumbers in **Figure 6**.

Figure 6

In this case, the higher the selectivity ratio is, the better the interval. The chosen intervals are framed with dotted red squares: 8728 – 8462 cm^{-1}, 7378 – 7112 cm^{-1}, 6032 – 4682 cm^{-1} (1146-1182 nm, 1355 – 1406 nm, 1658 – 2136 nm). These 490 variables were used for the creation of a new calibration model. Before the creation of this calibration model, the first derivatives were calculated for our dataset. Six PLS components were kept in the PLS model. The predicted **Y** values are plotted against the measured **Y** values on the **Figure 7**. The R^2 value of the calibration was 0.90 and the Q^2 value of the validation was 0.87. The RMSEC value was 8.90 (mg/g) and the RMSECV value was 10.85 (mg/g). The created model was comparable to the iPLS variable selected model and much better than the original one.

Figure 7

The selected spectra areas can be also assigned to functional groupings. Beyond the previous: methyl antisymmetric and symmetric C-H stretching vibrations (2^{nd} overtone), methylene antisymmetric and symmetric C-H stretching vibrations (2^{nd} overtone), methyl and methylene combined stretch and bend vibrations [31,32].

The result of GA

The genetic algorithm (GA) was the last applied variable selection method in the study. PLS Toolbox 7.9 (Eigenvector Research, Inc., Wenatchee, WA, USA) was used for the analysis. In the first step the variable selection was tried for the variables without any intervals. The following options were used for GA: the size of the population was 160 and the percentage of the initial terms which specifies the approximate number of variables included in the initial variable subsets was 30. The number of the maximum generation was 100 (the default value was left.). The mutation rate was 0.005, and double cross-over was used. In the case of double cross-over the overlap is higher between the parent and child genes. Cross-validation with five splits and data preprocessing (autoscaling of the **X** variables) was also used. Root mean squared error of cross-validation was selected as objective function for genetic algorithm.

When selecting individual wavelengths (i.e. variable intervals were not used), meaningful physical assignment of the wavelengths is impossible. It is presented on Figure S1 in the supplementary material. Thus, it confirmed the earlier statement of Andersen and Bro [25], that the genetic algorithm for individual wavelengths cannot produce appropriate results.

The biggest problem is that the number of variables is too large and the important variables cannot be selected. The connection between the wavenumbers cannot be taken into account reliably.

In the second case, variable windows (intervals) were used as recommended by ref. [25] and the width of the window was fifty, which was the maximum value in PLS toolbox. Thus, we had 28 intervals. The other options were the same as in the previous case. **Figure 8** shows a much better and valuable model than the previous one. The frequency of inclusion was plotted against the

window numbers. The spectra can also be seen on the graph. The higher the frequency of inclusion of a window is, the better the variable window.

Figure 8

Seven windows were used for the further modeling, which means 350 variables. Before the modeling the first derivatives as data scaling were used for the dataset. **Figure 9** shows the final model with genetic algorithm variable selection method. The predicted **Y** values are plotted against the measured **Y** values. The calibration model is marked with blue color and the validated model is marked with red color. The created model is as good as the other variable selected models and also better than the first, original model.

Figure 9

Six PLS components were sufficient for the calibration, and the R^2 value was 0.91 for the calibration and Q^2 value was 0.88 for the validation. The RMSEC value was 8.48 (mg/g) for the calibration and RMSECV value was 10.22 (mg/g) for the validation.

The selected spectra areas can also be assigned to functional groupings. Beyond the previous functional groupings, there is a connection with the phenolic group vibration of the reduced form of the molecule and there are also C-C/C-H combined vibrations according to references [31,32].

Comparison of models

Sum of ranking differences was used for comparison of the models. This method works with a home-made Microsoft EXCEL VBA macro, which is available on the Internet:

http://aki.ttk.mta.hu/srd

The matrix contained fifty rows (samples) and seven columns, which included the three models' predicted **Y** values for the calibration and the validation. Experimental values are also included, because we wanted to know whether the models are better than the HPLC method.

The experimental data divide the models into good ones (they rationalize the information in the data better than the experiments) and bad ones (the latter have worse ranking than the experimental

ones) in case the row-average is chosen as reference for SRD ordering [36]. It can also be called as consensus in accordance with the maximum likelihood principle, which yields a choice of the estimator as the value for the parameter that makes the observed data most probable (the average) [37]. Not only the random errors are canceled by each other, but the bias of the methods, at least partially. The fact that the bias of various laboratories and measurement methods follow normal distribution is a well substantiated empirical finding [38].

SRD values are given in two scales. The first is the original one and the second is the scaled one denoted by SRD_{nor}. On the diagram (**Figure 10)** the scaled results are used, which makes the methods comparable. The scaled SRD values are between 0 and 100. The equation of the scaling:

$$SRD_{nor}=100SRD/SRD_{max}\,, \qquad (5)$$

Where SRD_{max} = the maximum of the SRD values for the actual variable (model).

Figure 10 shows that all of the created models are ranked better, than the experimental method and the best model is the iPLS variable selected one: both of the calibration and validated model. The figure is the zoomed form of the original plot. The random probability distribution (a Gauss like curve) cannot be seen in **Figure 10**, although it helps us decide whether the model is better or similar than the use of random numbers. All of the ranks for models and experimental values are better than the use of random numbers.

Figure 10

Validation of the ranking has also been carried out using seven-fold cross-validation. For the latter, the dataset was split into seven subsets and then each subset's SRD values were calculated. SRDs were calculated on the seven $6/7^{th}$ portion and the original SRD values define the uncertainty of the SRD values for each method. The box & whisker plot (**Figure 11**) shows the SRD ranges (minimum and maximum), the second and third quartiles (box in which the 50% of the data are located) and the median small box. **Figure 11** shows that the median of iPLS calibration model (iPLS_C) is very far away from the others, and the median of the validated iPLS (iPLS_V) model and GA calibration model (GA_C) are very close to each other (similarly to the SRD graph).

Figure 11

Sign and Wilcoxon tests verified that there is no significant difference between these two models.

External validation of the models

External validation (or test validation) is an essential part of every multivariate calibration model [39]. If it is possible it should be used, because the application of external, newly measured samples can verify the models most reliably.

The three calibration models were tested on six external samples, which have been received after the construction of our models. The same number of PLS components were used for the external validation of the interval PLS variable selected model as it was determined in the model building phase. The Q^2 value was 0.93 and the RMSEP (Root mean squared error of prediction) value was 8.82 (mg/g) for the validation. In the case of the interval SR variable selected model the Q^2 value was 0.83 and the RMSEP value was 13.74 (mg/g). Finally in the case of the GA variable selected model the Q^2 value was 0.89 and the RMSEP value was 11.12 (mg/g).

Discussion

Table 2 summarizes eleven calibration models created in this study, and three of them can be recommended for calibration. All variable selection methods are very useful in improving calibration models. Each of the best three selected models has higher R^2 value than 0.90 and higher Q^2 value than 0.86. The external validation of the final models was successful. The parameters of the models are as good as in the case of internal (cross) validation. Derivative data scaling can be considered as the best data pretreatment method for this spectra dataset. SRD method verified that all of the created methods are suitable for the further analysis of CoQ10 samples.

The final conclusion is that each of the three improved models is capable of the determination of CoQ10 samples' concentrations. The FT-NIRS method combined with PLS-R and variable selection techniques is a very good option to open the way to fast, simple and reliable calibration models.

Acknowledgement

The investigations were supported by the Hungarian Scientific - Research Foundation OTKA No K112547. We are indebted to BioCo Magyarország company for providing the CoQ10 samples.

References

1. Ernster L, Dallner G (1995) Biochemical, physiological and medical aspects of ubiquinone function. Biochim Biophys Acta 1271:195–204.

2. Hargreaves IP (2014) Coenzyme Q10 as a therapy for mitochondrial disease. Int J Biochem Cell Biol 49:105–111.

3. Lockwood K, Moesgaard S, Yamamoto T, Folkers K (1995) Progress on therapy of breast cancer with vitamin Q10 and the regression of metastases. Biochem Biophys Res Commun 212:172–177.

4. Lee B-J, Huang Y-C, Chen S-J, Lin P-T (2012) Coenzyme Q10 supplementation reduces oxidative stress and increases antioxidant enzyme activity in patients with coronary artery disease. Nutrition 28:250–255.

5. Fotino AD, Thompson-Paul AM, Bazzano LA (2013) Effect of coenzyme Q10 supplementation on heart failure: a meta-analysis. Am J Clin Nutr 97:268–275.

6. Belardinelli R, Muçaj A, Lacalaprice F, et al. (2006) Coenzyme Q10 and exercise training in chronic heart failure. Eur Heart J 27:2675–2681.

7. López-Lluch G, Rodríguez-Aguilera JC, Santos-Ocaña C, Navas P (2010) Is coenzyme Q a key factor in aging? Mech Ageing Dev 131:225–235.

8. Mattila P, Kumpulainen J (2001) Coenzymes Q9 and Q10: Contents in foods and dietary intake. J Food Compos Anal 14:409–417.

9. Breithaupt DE, Kraut S (2006) Simultaneous determination of the vitamins A, E, their esters and coenzyme Q10 in multivitamin dietary supplements using an RP-C30 phase. Eur Food Res Technol 222:643–649.

10. Lang JK, Packer L (1987) Quantitative determination of vitamin E and oxidized and reducted coenzyme Q by high-performance liquid chromatography with in-line ultraviolet and electrochemical detection. J Chromatogr 385:109–117.

11. Tang PH, Miles M V, DeGrauw A, et al. (2001) HPLC analysis of reduced and oxidized coenzyme Q10 in human plasma. Clin Chem 47:256–265.

12. Ratnam DV, Bhardwaj V, Kumar MNVR (2006) Simultaneous analysis of ellagic acid and coenzyme Q10 by derivative spectroscopy and HPLC. Talanta 70:387–391.

13. Lunetta S, Roman M, Chandrah A, et al. (2008) Determination of coenzyme Q10 content in raw materials and dietary supplements by high-performance liquid chromatography-UV: Collaborative study. J AOAC Int 91:702–708.

14. Lee JH, Hoang NH, Huong NL, et al. (2014) Ultra-performance liquid chromatography with electrospray ionization mass spectrometry for the determination of coenzyme Q10 as an anti-aging ingredient in edible cosmetics. Anal Lett 47:367–376.

15. Rodríguez-Acuña R, Brenne E, Lacoste F (2008) Determination of coenzyme Q10 and Q9 in vegetable oils. J Agric Food Chem 56:6241–6245.

16. Monakhova YB, Ruge I, Kuballa T, et al. (2013) Rapid determination of coenzyme Q10 in food supplements using 1H NMR spectroscopy. Int J Vitam Nutr Res 83:67–72.

17. Fodor M, Woller A, Turza S, Szigedi T (2011) Development of a rapid, non-destructive method for egg content determination in dry pasta using FT-NIR technique. J Food Eng 107:195–199.

18. Magwaza LS, Opara UL, Terry L a., et al. (2013) Evaluation of Fourier transform-NIR spectroscopy for integrated external and internal quality assessment of Valencia oranges. J Food Compos Anal 31:144–154.

19. Martínez-Aguilar JF, Ibarra-Montaño EL (2007) Complete quality analysis of commercial surface-active products by Fourier-transform near infrared spectroscopy. Talanta 73:783–790.

20. Sáiz-Abajo M-J, González-Sáiz J-M, Pizarro C (2005) Orthogonal signal correction applied to the classification of wine and molasses vinegar samples by near-infrared spectroscopy. Feasibility study for the detection and quantification of adulterated vinegar samples. Anal Bioanal Chem 382:412–20.

21. Huang H, Yu H, Xu H, Ying Y (2008) Near infrared spectroscopy for on/in-line monitoring of quality in foods and beverages: A review. J Food Eng 87:303–313.

22. Cocchi M, Durante C, Foca G, et al. (2006) Durum wheat adulteration detection by NIR spectroscopy multivariate calibration. Talanta 68:1505–1511.

23. Vass A, Deák E, Dernovics M (2014) Quantification of the reduced form of coenzyme Q10, ubiquinol, in dietary supplements with HPLC-ESI-MS/MS. Food Anal Methods. doi: 10.1007/s12161-014-9911-x

24. Geladi P, Kowalski BR (1986) Partial least-squares regression: a tutorial. Anal Chim Acta 185:1–17.

25. Andersen CM, Bro R (2010) Variable selection in regression-a tutorial. J Chemom 24:728–737.

26. Nørgaard L, Saudland A, Wagner J, et al. (2000) Interval partial least-squares regression (iPLS): A comparative chemometric study with an example from near-infrared spectroscopy. Appl Spectrosc 54:413–419.

27. Kristensen M, Savorani F, Ravn-Haren G, et al. (2009) NMR and interval PLS as reliable methods for determination of cholesterol in rodent lipoprotein fractions. Metabolomics 6:129–136.

28. Di Anibal CV, Callao MP, Ruisánchez I (2011) 1H NMR variable selection approaches for classification. A case study: the determination of adulterated foodstuffs. Talanta 86:316–323.

29. Rajalahti T, Arneberg R, Berven FS, et al. (2009) Biomarker discovery in mass spectral profiles by means of selectivity ratio plot. Chemom Intell Lab Syst 95:35–48.

30. Leardi R (2007) Genetic algorithms in chemistry. J Chromatogr A 1158:226–233.

31. Héberger K (2010) Sum of ranking differences compares methods or models fairly. TrAC Trends Anal Chem 29:101–109.

32. Héberger K, Kollár-Hunek K (2011) Sum of ranking differences for method discrimination and its validation: comparison of ranks with random numbers. J Chemom 25:151–158.

33. Kollár-Hunek K, Héberger K (2013) Method and model comparison by sum of ranking differences in cases of repeated observations (ties). Chemom Intell Lab Syst 127:139–146.

34. Workman J, Jr. (2000) Functional groupings and calculated locations in wavenumbers (cm-1) for IR spectroscopy. In: Handb. Org. Compd. Academic Press, pp 229–236

35. Workman J, Jr., Weyer L (2007) Practical Guide to Interpretive Near-Infrared Spectroscopy. CRC Press, p 344.

36. Héberger K, Skrbić B (2012) Ranking and similarity for quantitative structure-retention relationship models in predicting Lee retention indices of polycyclic aromatic hydrocarbons. Anal Chim Acta 716:92–100.

37. Hastie T, Tibshirani R, Friedman J (2001) Overview of Supervised Learning. In: Elem. Stat. Learn. Data Mining, Inference, Predict. Springer, New York, p 31

38. Youden WJ (1975) Statistical Manual of the Association of Official Analytical Chemists: Statistical Techniques for Collaborative Test. AOAC International, Gaithersburg

39. Esbensen KH, Geladi P (2010) Principles of proper validation: Use and abuse of re-sampling for validation. J Chemom 24:168–187.

Table 1: Summary of used methods for CoQ10 content determination

Name	Method	Matrix	Components	Other
D. E. Breaithaupt *et. al.*[9]	RP-HPLC/DAD and LC-(APCI)MS for identification	dietary supplements	vitamins A, E and Q10	LOQ_{UV}= 0.7 µg/mL
J. K. Lang *et. al.*[10]	RP-HPLC - UV and Electrochemical detector	blood, plasma and other tissues	vitamin E isomers, Q10 and Q9 (oxidized and reduced form)	LOD(Q9,10)= 1 pmol
P. H. Tang *et. al.*[11]	RP-HPLC - coulometric detection	human plasma	Q10 (reduced and oxidized form)	Analytical recovery= 95.8-101.0 %
D. V. Ratnam *et. al.*[12]	fist derivative UV spectroscopic and HPLC/DAD (PEG bonded column)	in solution	ellagic acid and Q10	Accuracy(Q10)= 101.83 % Precision(Q10)= 3.36 %
S. Lunetta *et. al.*[13]	HPLC-UV	raw materials and dietary supplements	Q10	Recovery= 74.0-115 %
J. H. Lee *et. al.*[14]	UPLC-ESI-MS/MS	edible cosmetics	Q10	LOD= 100 ng/mL
R. Rodrígez-Acuña *et. al.*[15]	HPLC-MS	vegetable oils	Q10 and Q9	LOQ= 0.025 mg/kg
Y. B. Monakhova *et. al.*[16]	^{1}H NMR	dietary supplements	Q10	LOD= 7.8 mg/L

Table 2: Performance parameters, scaling methods and number of latent variables of the models. MSC - multiplicative scatter correction.

	R^2	Q^2	RMSEC	RMSECV	Scaling	No. Comp.	Variable selection
1.	0.85	0.71	11.26	15.74	No	9	No
2.	0.90	0.53	8.91	19.93	derivative	9	No
3.	0.88	0.80	9.94	13.14	autoscale	8	No
4.	0.89	0.74	9.69	15.68	MSC	8	No
5.	0.91	0.72	8.63	15.45	MSC+derivative	10	No
6.	**0.92**	**0.87**	**8.16**	**10.58**	**derivative**	**7**	**iPLS**
7.	0.88	0.78	9.97	14.03	MSC	7	iPLS
8.	0.89	0.82	9.68	12.12	autoscale	8	iPLS
9.	**0.90**	**0.87**	**8.90**	**10.85**	**derivative**	**6**	**iSR**
10.	**0.91**	**0.88**	**8.48**	**10.22**	**derivative**	**6**	**GA**

Figure 1: The graph of the average and the two outlier NIR spectra (absorbance was plotted against wavenumbers).

Figure 2: The score plot of the PCA for the outlier detection. 99% confidence interval is marked by dashed line (PC Score 3 against PC Score 1 was plotted).

Figure 3: The base calibration model without any data pretreatment and variable selection. The calibration samples are denoted by empty circles whereas full circles mean validation samples.

Figure 4: RMSECV values (for each interval) are plotted against the wavenumbers. The spectrum is marked with yellow and the RMSECV value for all of the dataset is marked with blue dashed line. The important variables are marked with red dashed square.

Figure 5: Calibration and validated model with interval PLS variable selection and derivative data scaling.

Figure 6: Selectivity ratio values for each interval (Eq. (4), the higher the better) are plotted against the wavenumbers. Important variables are marked with red dashed squares.

Figure 7: Calibration and validated model with variable selection using interval selectivity ratio and derivative data scaling.

Figure 8: The frequency of inclusion (the higher the better) against the window of variables. The average spectrum is marked with a red line. The important variables are marked with orange dashed squares.

Figure 9: Calibration and validated model with genetic algorithm variable selection and derivative data scaling.

Figure 10: Sum of ranking differences for the model comparison. Relative frequency % of the random numbers is connected to the Gauss-like curve (The Gauss curve is omitted for clarity). Notations: IPLS_C and IPLS_V mean the calibration and validation models with interval PLS variable selection. iSR_C and iSR_V mean the calibration and validation models with interval SR

variable selection. GA_C and GA_V mean the calibration and validation models with interval GA variable selection. Exp means experimental values determined by HPLC.

Figure 11: Box & whisker plot of sum of ranking differences (seven-fold cross-validation).

Figure 1

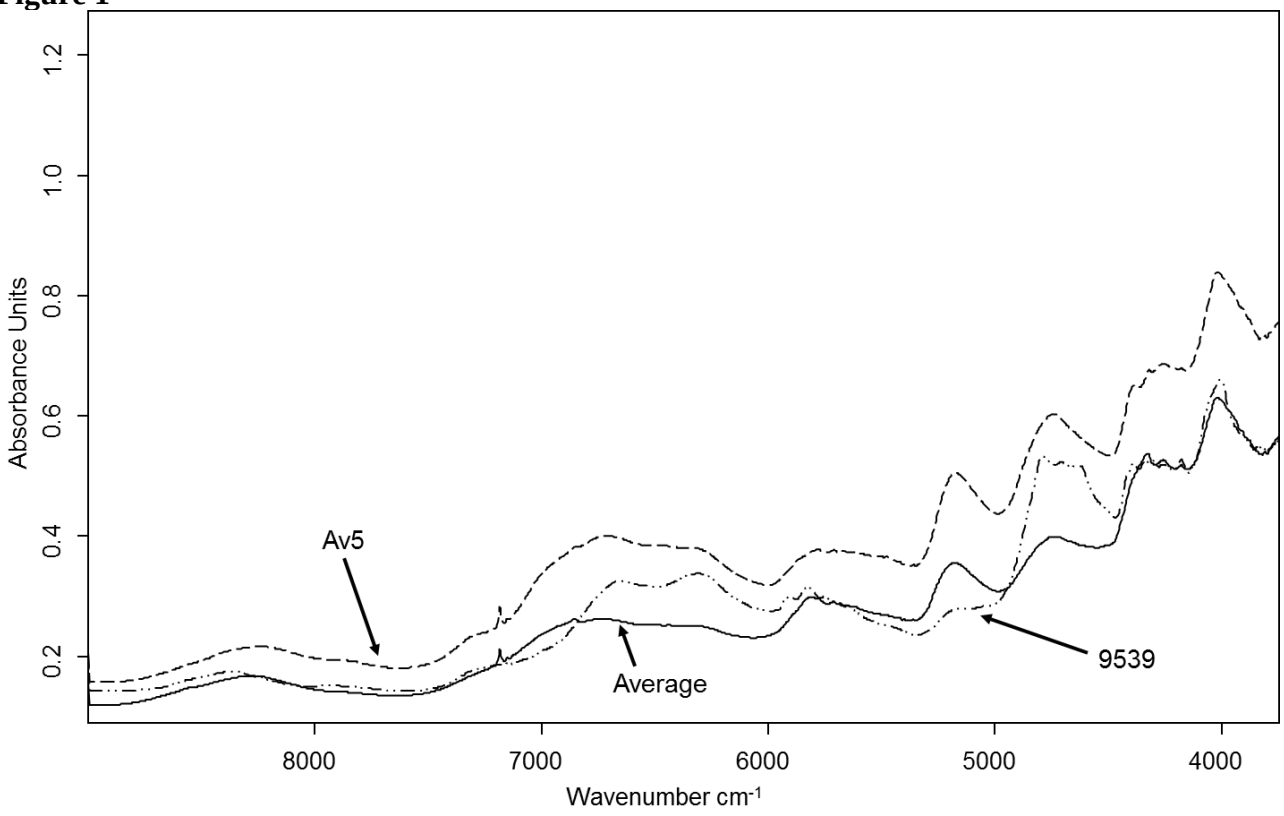

Figure 2

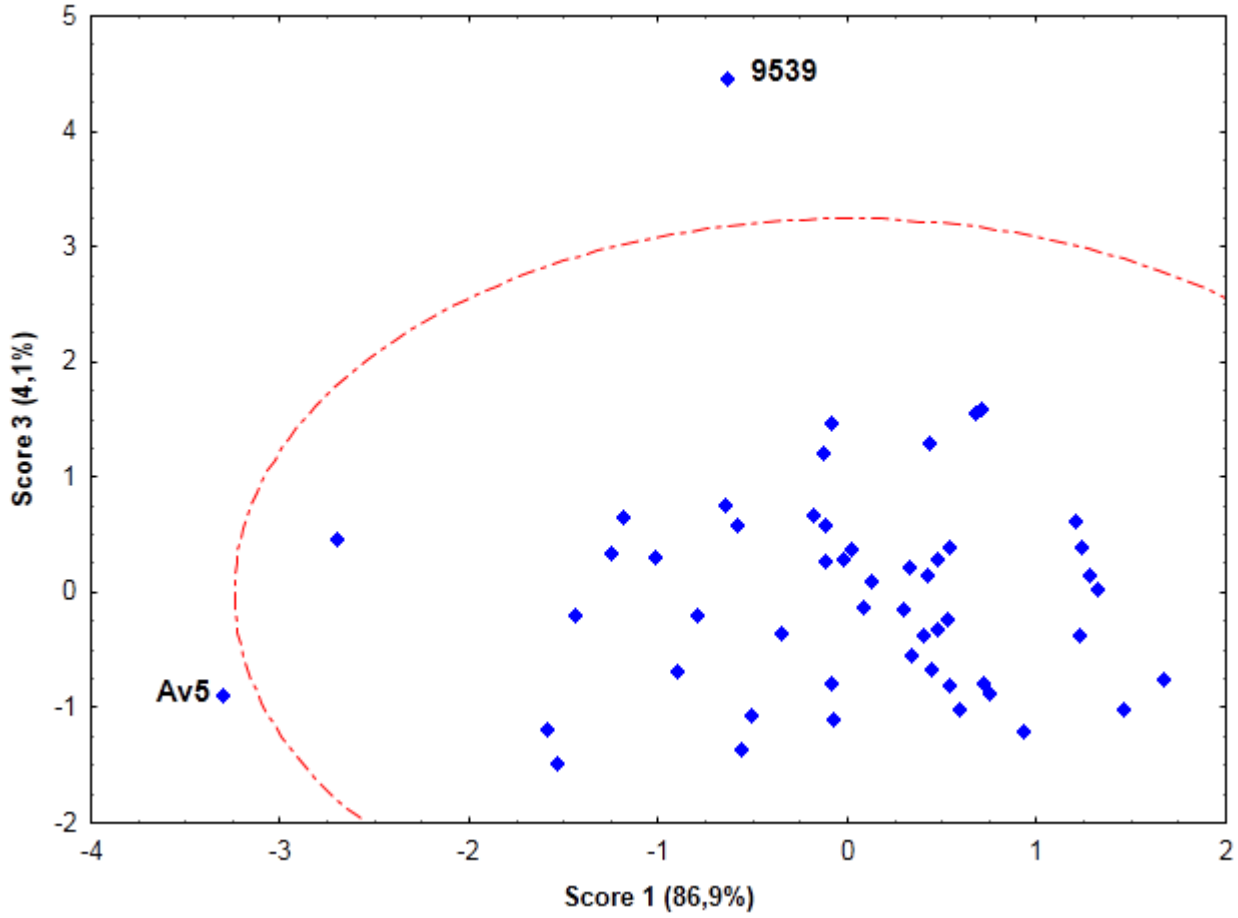

Figure 3

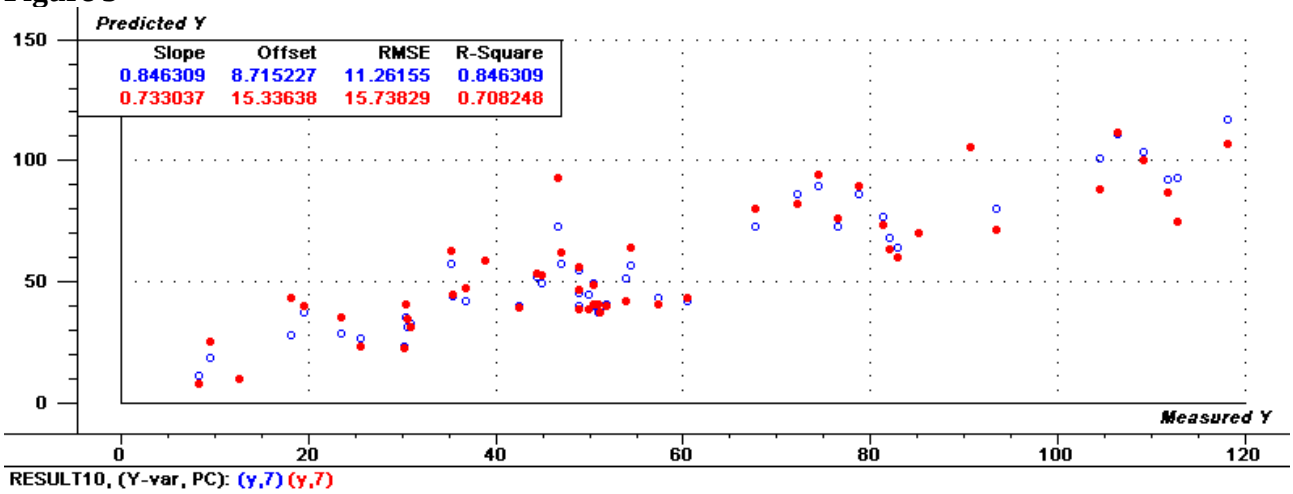

Figure 4

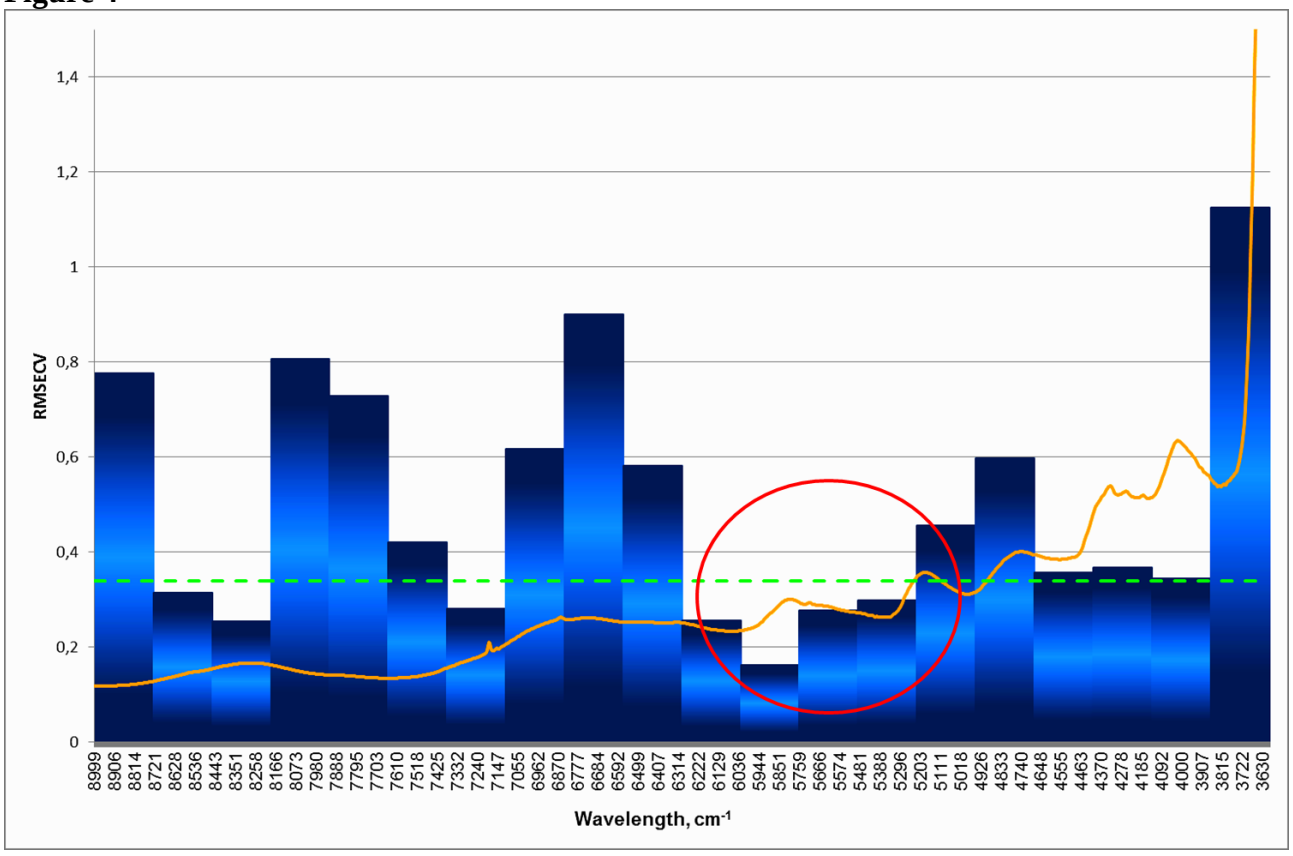

Figure 5

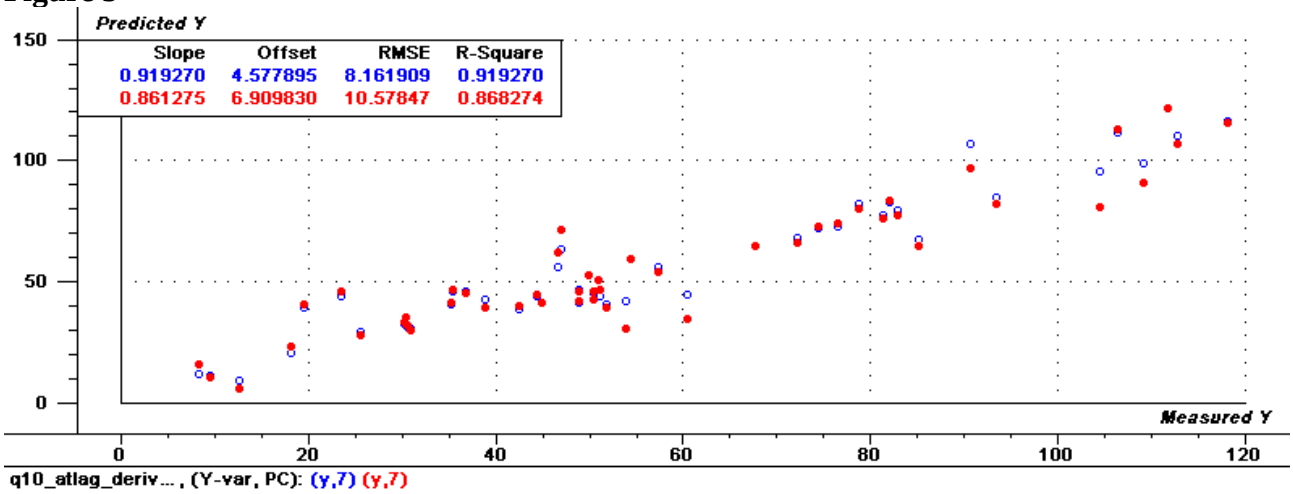

Figure 6

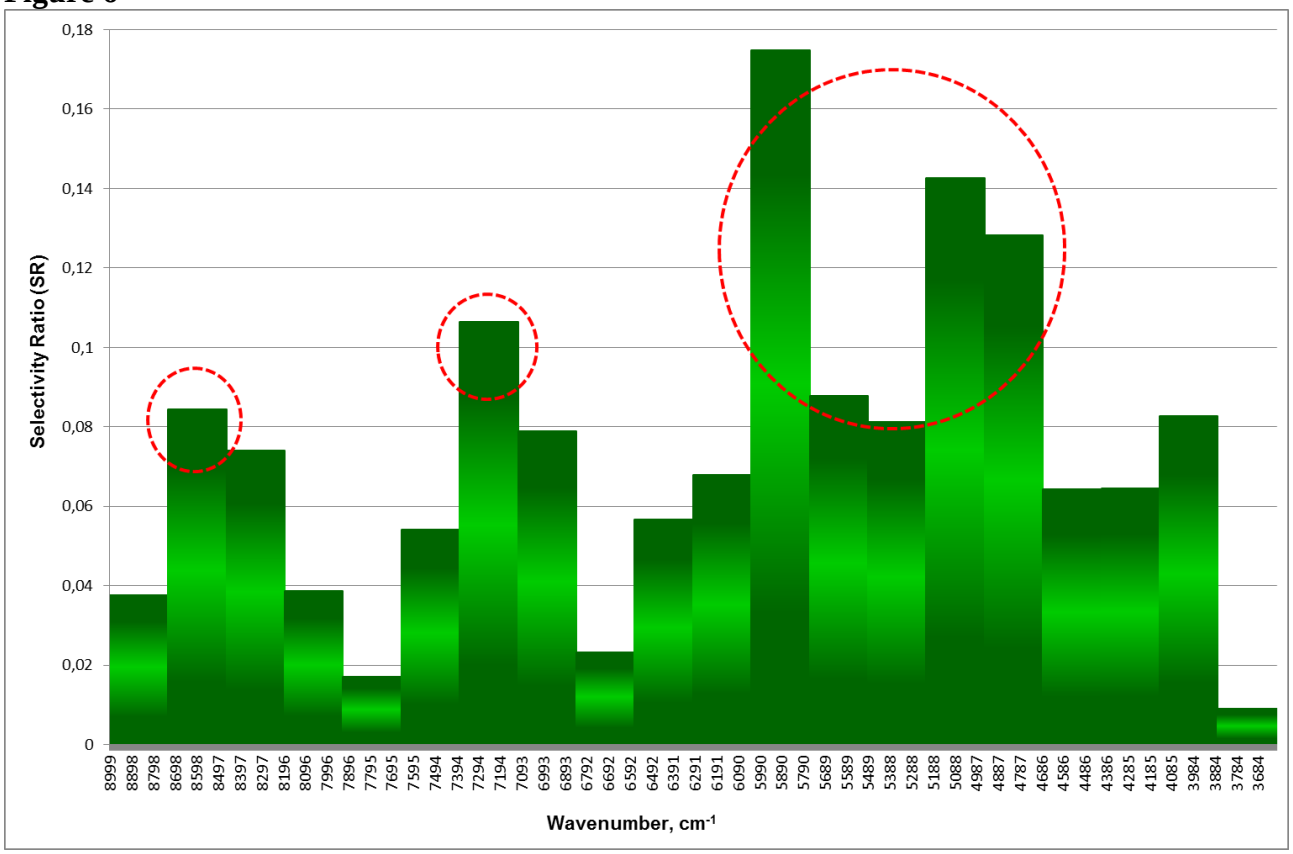

Figure 7

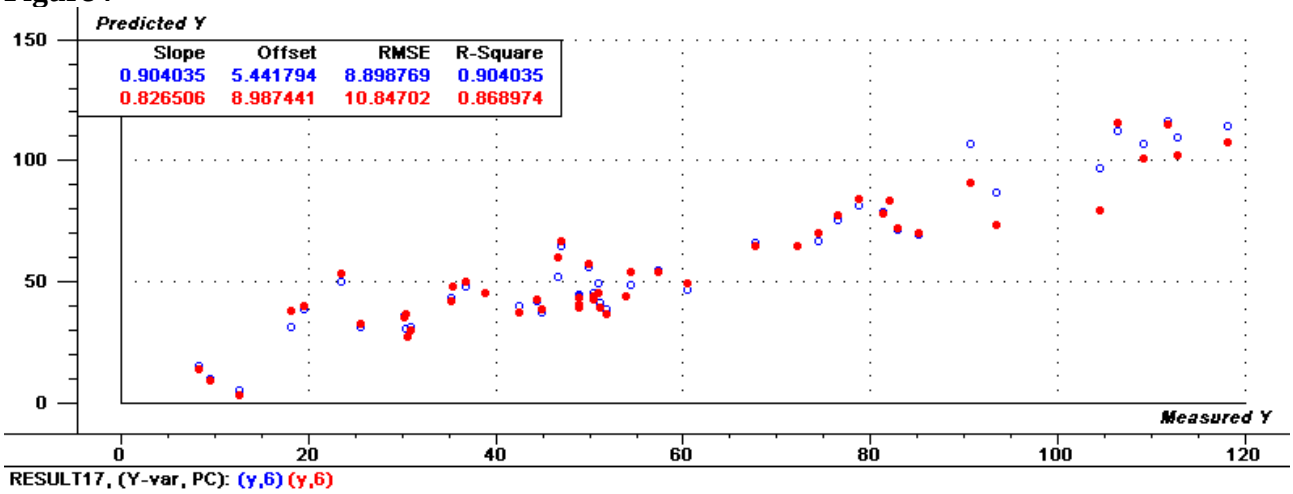

Figure 8

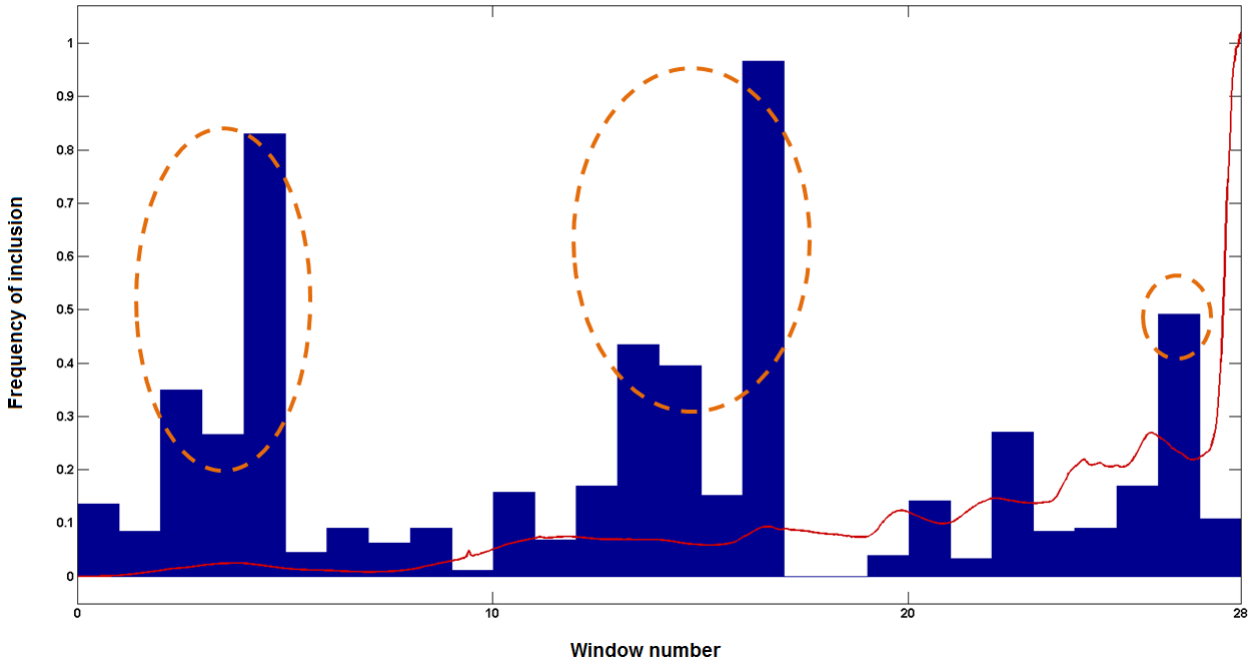

Figure 9

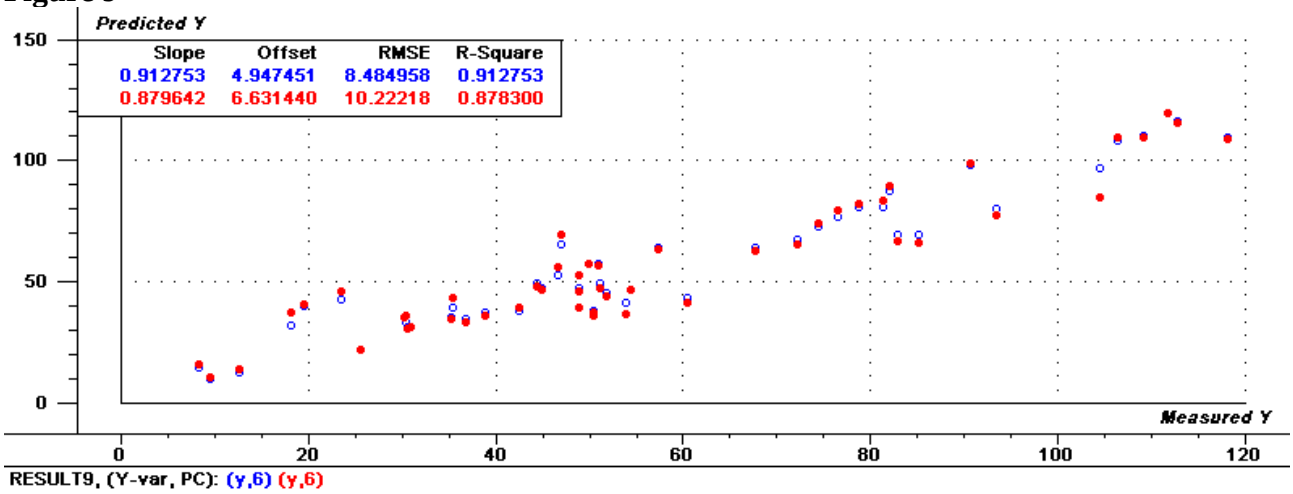

Figure 10

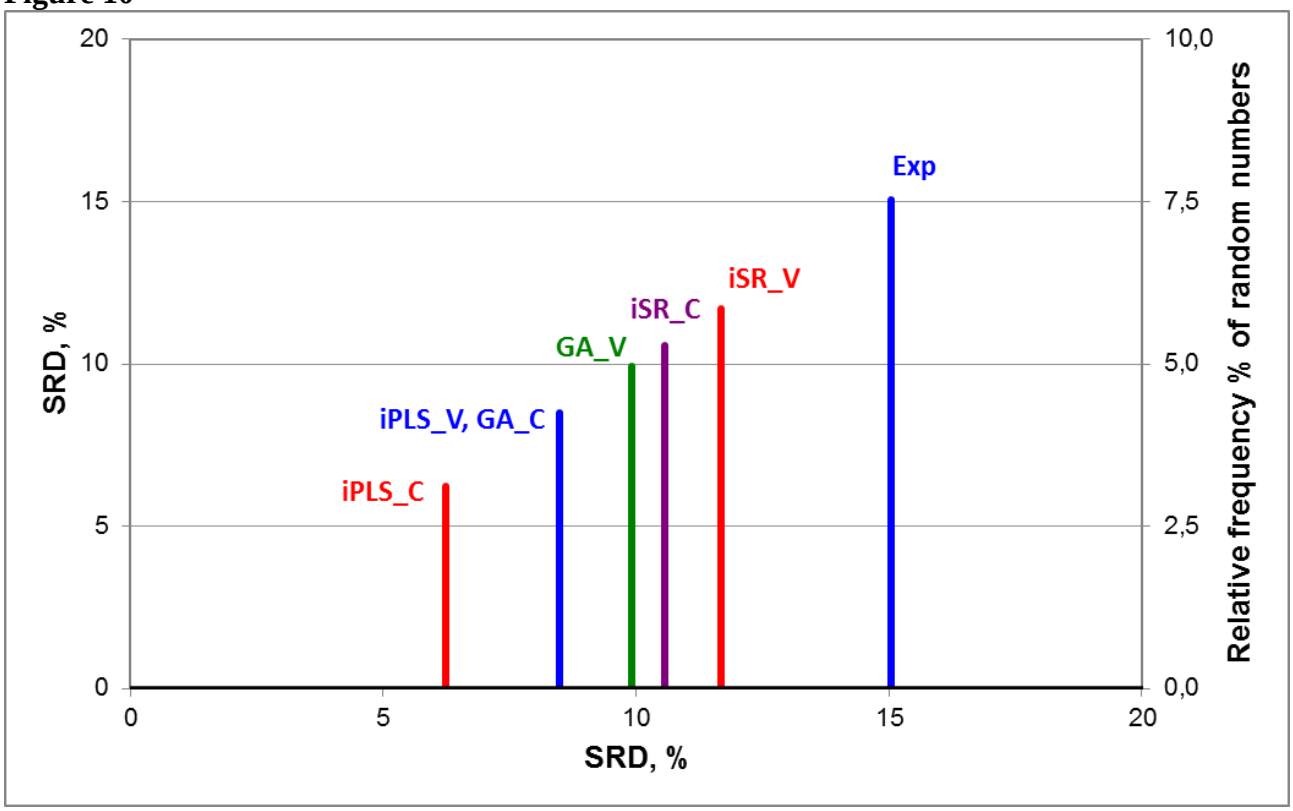

Figure 11

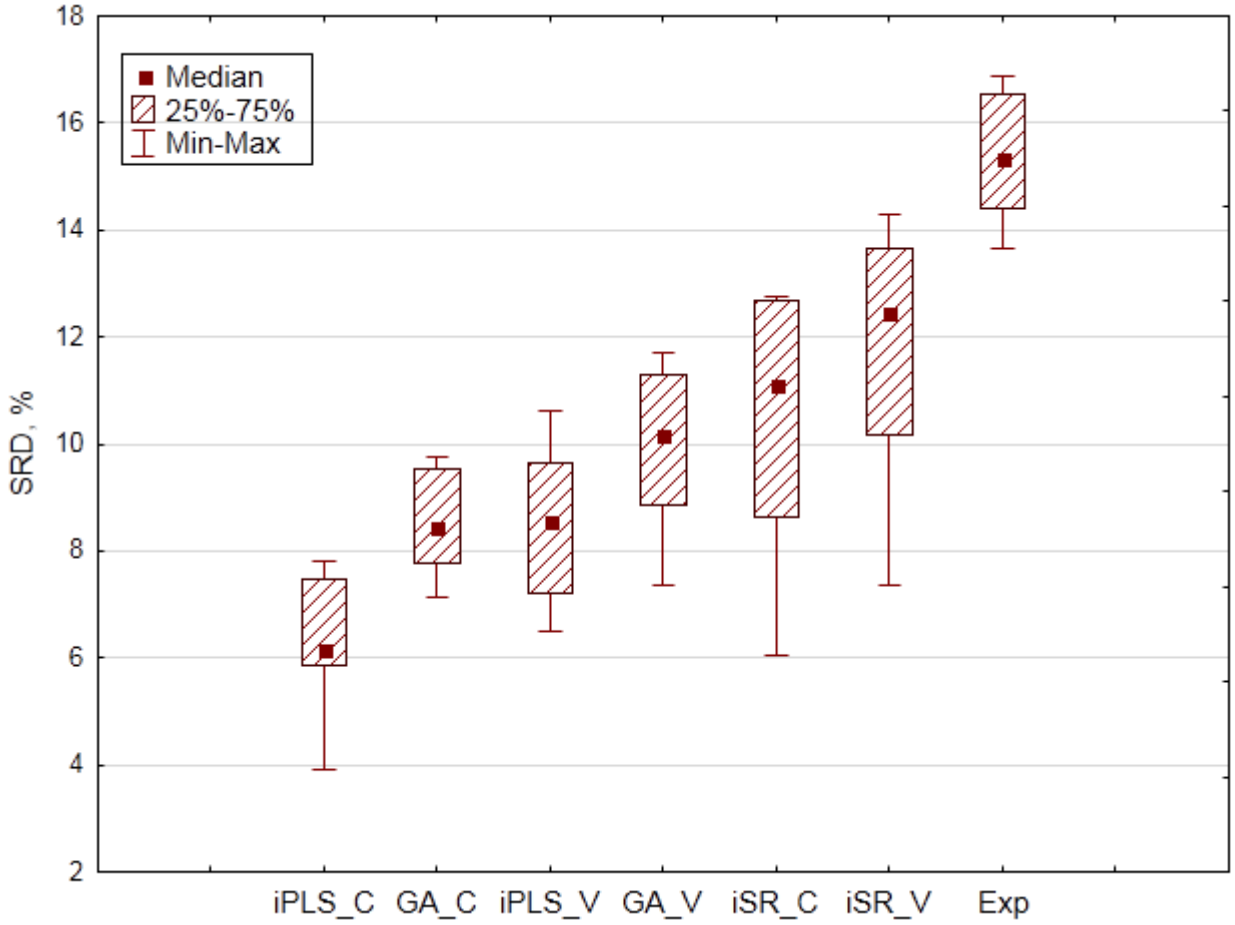

Online abstract figure

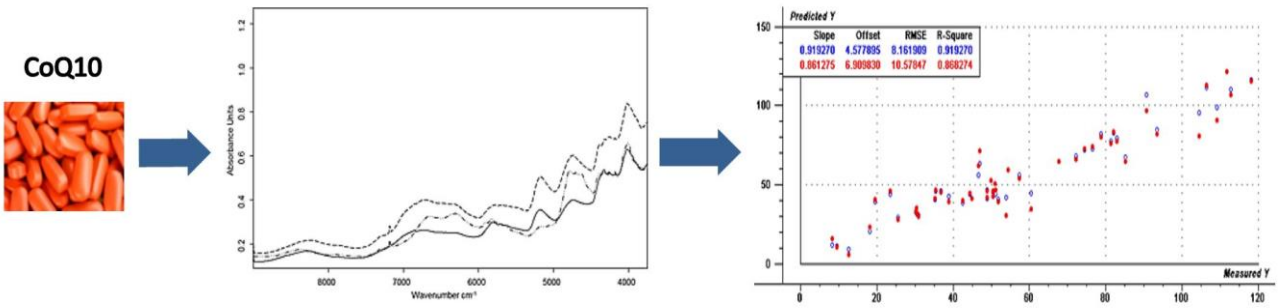

Quantitative Determination of Coenzyme Q_{10} from Dietary Supplements by FT-NIR Spectroscopy and Statistical Analysis

Anita Rácz[1,2], Andrea Vass[2], Károly Héberger[1,*], Marietta Fodor[2]

[1] Research Centre for Natural Sciences, Hungarian Academy of Sciences, Institute of Materials and Environmental Chemistry, Department of Plasma Chemistry

H-1117 Budapest XI., Magyar Tudósok krt. 2.

[2] Corvinus University of Budapest, Faculty of Food Science, Department of Applied Chemistry,

H-1118 Budapest XI., Villányi út 29-43.

* To whom correspondence should be sent:

E-mail address: heberger.karoly@ttk.mta.hu (Károly Héberger)

Phone: +36 1 382 6509

Figure S1: The frequency of inclusion for each variable (variable importance) according to individual selection by genetic algorithm. When selecting individual wavelengths (i.e. variable intervals were not used), meaningful physical assignment of the wavelengths is impossible.